6026 *Inorg. Chem.* **2009**, *48*, 6026–6033
DOI: 10.1021/ic9003406

Inorganic Chemistry
Article

2D and 3D Polymeric Wells–Dawson Polyoxometelates: Synthesis, Crystal Structures, and Cyclic Voltammetry of $[(M(H_2O)_4)_x][H_{6-2x}P_2W_{18-n}Mo_nO_{62}]$ ($M = Cu^{II}$, Co^{II}, Ni^{II})

Robila Belghiche,[†] Ouahiba Bechiri,[†] Mostefa Abbessi,*[,†] Stéphane Golhen,[‡] Yann Le Gal,[‡] and Lahcène Ouahab*[,‡]

[†]*Laboratoire de Recherche Génie de l'Environnement, Département de Génie des Procédés, Faculté des Sciences de l'Ingénieur, Université Badji Mokhtar, BP12 Annaba, Algérie, and* [‡]*Organométalliques et Matériaux Moléculaires, UMR 6226 CNRS–Université de Rennes 1, Sciences Chimiques de Rennes, Avenue Général Leclerc, 35042 Rennes Cedex, France*

Received February 19, 2009

The synthesis, X-ray crystal structures, cyclic voltammetry, and IR and ^{31}P NMR characterizations of five new Wells–Dawson-type polyoxometalates are reported, the formulas of which being $[(Cu(H_2O)_4)_{2.5}][HP_2W_{18}O_{62}]\cdot 11.33H_2O$ (**4**), $[(Cu(H_2O)_4)_{2.4}][H_{1.2}P_2W_{12}Mo_6O_{62}]\cdot 11.4H_2O$ (**5**), $[(Cu(H_2O)_4)_{2.3}][H_{1.4}P_2W_{15}Mo_3O_{62}]\cdot 10.1H_2O$ (**6**), $[Co(H_2O)_4)_{2.3}][H_{1.4}P_2W_{14}Mo_4O_{62}]\cdot 18.8H_2O$ (**7**), and $[Ni(H_2O)_4)_{1.85}][H_{2.3}P_2W_{15}Mo_3O_{62}]\cdot 20.6H_2O$ (**8**). These compounds are obtained as crystalline materials from the corresponding acids by substitution of a transition metal in aqueous solution. Compounds **4**, **5**, and **6** are isostructural; their crystal structure consists of 2D polymeric hexagonal layers where each Wells–Dawson anion is connected to six neighbors by $[CuO_6]$ octahedra. On the other hand, compounds **7** and **8**, which are also isostructural, present a 3D structure where the Mo-substituted $[P_2W_{14}Mo_4O_{62}]$ units are connected by $[MO_6]$ octahedra ($M = Co^{II}$, Ni^{II}). Different types of substitution modes of Mo ions are observed within polyanions. Cyclic voltammetry shows that Cu^{II} derivatives have similar behavior but different from that of the starting compounds. No electrochemical activity has been detected for the Ni-containing compound **8**.

Introduction

Heteropolyanions or polyoxometalates (POMs) are metal oxide clusters of general formula $[XM_pO_q]^{n-}$, where X represents a heteroatom and M a 4d or 5d transition metal ion. They have a great deal of structural diversity[1−8] and various applications in different areas, including catalysis,[9] material sciences,[10] medicine, and biology.[11] Several types have been characterized, and each of them is defined by the M/X ratio used in the polycondensation under acidic conditions. The two best known heteropolyanions are the Keggin-type $[XM_{12}O_{40}]^{n-}$ with M/X ratios = 12[1,2] and 9, the latter ones called the Wells-Dawson type $[(X^{n+})_2M_{18}O_{62}]^{(16-2n)-}$.[3−5] The latter is composed of two lacunar Keggin anions $[XM_9O_{34}]^{9-}$ linked together, leading to the $[X_2M_{18}O_{62}]^{6-}$ species. It is worth mentioning that the phospho-tungstic potassium salt $K_6[P_2W_{18}O_{62}]\cdot 20H_2O$, for example, leads by stereospecific alkaline degradation and, depending on the pH, to the $[P_2W_{17}O_{61}]^{10-}$ monovacant species,[5] the trivacant $[P_2W_{15}O_{56}]^{10-}$ species,[6] or the hexavacant $[P_2W_{12}O_{48}]^{12-}$ species.[6] These compounds are subject to addition reactions, yielding new monovacant species such as $[P_2W_{15}Mo_2O_{61}]^{10-}$,[3,4] $[P_2W_{12}Mo_5O_{61}]^{10-}$,[7] or saturated mixed species such as $[P_2W_{12}Mo_6O_{62}]^{6-}$.

The intrinsic property of lacunar compounds to give mixed complexes by the addition of 3d metallic elements has been widely investigated in order to prepare compounds of formulas $[M'(OH_2)P_2W_{12}Mo_5O_{61}]^{8-}$ and $[M'(OH_2)P_2W_{15}Mo_2O_{61}]^{8-}$ (M' = Ni, Cu, Co, etc.) with the divalent elements.[3−5,7] On the other hand, it has been shown that the extraction of the acidic form of the saturated species by the etherate method is quite possible and leads to $H_6P_2W_{18}O_{62}\cdot 24H_2O$, $H_6P_2W_{12}Mo_6O_{62}\cdot 24H_2O$, and $H_6P_2W_{15}Mo_3O_{62}\cdot 24H_2O$.[8,12]

*To whom correspondence should be addressed. E-mail: abbessi_mostefa@yahoo.fr (M.A.), lahcene.ouahab@univ-rennes1.fr. (L.O.).

(1) Zhang, Q.-Z.; Lu, C.-Z.; Yang, W.-B.; Wu, C.-D.; Yu, Y.-Q.; Yan, Y.; Liu, J.-H.; He, X. *J. Cluster Sci.* **2003**, *09*(3), 381–390.
(2) Contant, R.; Thouvenot, R. *Can. J. Chem.* **1991**, *69*, 1498–1506.
(3) Abbessi, M.; Contant, R.; Thouvenot, R.; Hervé, G. *Inorg. Chem.* **1991**, *30*, 1695–1702.
(4) Contant, R.; Abbessi, M.; Canny, J.; Richet, M.; Keita, B.; Belhouari, A.; Nadjo, L. *Eur. J. Inorg. Chem.* **2000**, 567–574.
(5) Keita, B.; Girard, B.; Nadjo, L.; Contant, R.; Canny, J.; Richet, M. *J. Electroanal. Chem.* **1999**, *478*, 76–82.
(6) Contant, R.; Ciabrini, J. P. *J. Org. Nucl. Chem.* **1981**, *43*, 1525–1528.
(7) Belghiche, R.; Contant, R.; Lu, Y. W.; Keita, B.; Abbessi, M.; Nadjo, L.; Mahuteau *Eur. J. Inorg. Chem.* **2002**, 1410–1414.
(8) Contant, R. *Inorg. Synth.* **1990**, *27*, 104–111.
(9) Briand, L. E.; Baronetti, G. T.; Thomas, H. J. *Appl. Catal., A* **2003**, *256*(1−2), 37–50.
(10) (a) Boglio, C.; Lemière, G.; Hasenknop, B.; Thorimbert, S.; Lacôte, E.; Malacria, M. *Angew. Chem., Int. Ed.* **2006**, *45*, 3324–3327. (b) Yin, C. X.; Finke, R. G. *J. Am. Chem. Soc.* **2005**, *127*, 9003–9013.
(11) Witvrouw, M.; Weigold, H.; Pannecouque, C.; Schols, D.; Clercq, E. D.; Holan, G. *J. Med. Chem.* **2000**, *43*, 778–783.
(12) Abbessi, M. Thèse de Doctorat, Université Pierre et Marie Curie, Paris VI, Paris, 1989.

Published on Web 06/09/2009

It was shown also that the position of the metallic element introduced in lacunar species influences significantly the redox potential of the considered species.[13] The introduction of metallic elements into the environment of the saturated species and the determination of their position by X-ray diffraction structure analysis have not been really investigated yet. Therefore, it would be interesting to compare the effect of this modification on the physical and chemical properties of the obtained species. Additionally, it might be judicious to prepare the heterometallic compounds from the acidic form. In fact, it was reported in a recent study that the proton of the acidic form of saturated species could be exchanged with a cobalt ion through a polymeric membrane.[14] Thus, this route will be explored to synthesize the target products. Once synthesized, the Dawson-type structures and their derivatives were often deduced from ^{31}P NMR and recently refined by ^{183}W NMR measurements.[15] The analysis of their IR spectra has shown that some metallic ions fit into the cavities, while others remain outside the cavity. Wells−Dawson POMs have been investigated as catalysts; however, information on their catalytic properties is scarce.[9] A recent catalytic study based on the reduction potentials and UV−visible absorption edge energies of mixed W/Mo Wells−Dawson heteropolyacids has been reported.[16] The present work focuses on the addition of divalent metal ions to the $[H_6P_2W_{18}O_{62}]\cdot 24H_2O$ and $[H_6P_2W_{18-n}Mo_nO_{62}]\cdot 24H_2O$ (n = 3, 6) acidic forms in order to study the effect of the nature of the added element on the physicochemical properties of the synthesized complexes. In a subsequent step, we are planning to investigate the correlation between catalytic properties and structural features of this kind of POM.

Experimental Section

Synthesis and IR and ^{31}P NMR Spectroscopy. The heteropolyanion precursors $[H_6P_2W_{18}O_{62}]\cdot 24H_2O$ (**1**), $[H_6P_2W_{12}Mo_6O_{62}]\cdot 24H_2O$ (**2**), and $[H_6P_2W_{15}Mo_3O_{62}]\cdot 24H_2O$ (**3**) were synthesized according to published procedures,[6,17,18] and their purity was confirmed by ^{31}P NMR spectroscopy. The IR spectra were recorded on KBr pellets using a Shimadzu FTIR-8400s spectrophotometer. ^{31}P NMR spectra were recorded on a Bruker 2000 apparatus operating at 110 MHz in the Fourier transform mode. The ^{31}P shifts were measured for 10^{-3} M solutions of polyanions in D_2O solution and were referenced to 85% H_3PO_4. Elemental analyses were determined with a SPECTRO CIROS VISION inductively coupled plasma (ICP) spectrometer. About 20 mg of the solid sample was dissolved in 25 mL of 2 vol % HNO_3 solution for each analysis.

$[(Cu(H_2O)_4)_{2.5}][HP_2W_{18}O_{62}]\cdot 11.33H_2O$ (4). A total of 0.556 g of solid $CuCl_2{,}2H_2O$ (3.26 mmol) was added to 20 mL of a water solution of 5 g (1.088 mmol) of $H_6P_2W_{18}O_{62}$ at room temperature. The mixture was then stirred for 10 min. Blue crystals of **4** suitable for X-ray diffraction were obtained after five days by slow evaporation, 70% yield. IR (KBr pellet, cm^{-1}): 1100(s), 1025(w), 960(s), 910(s). NMR of **4**. ^{31}P NMR: δ −12.36. Anal. calcd for **4**: Cu, 3.24; W, 67.44; P, 1.26. Found: Cu, 3.81; W, 62.91; P, 1.22.

$[(Cu(H_2O)_4)_{2.4}][H_{1.2}P_2W_{12}Mo_6O_{62}]\cdot 11.4H_2O$ (5). A total of 5 g (1.2 mmol) of $H_6P_2W_{12}Mo_6O_{62}$ was dissolved in 20 mL of water at room temperature, and 0.608 g (3.56 mmol) of solid $CuCl_2\cdot 2H_2O$ was then added. The mixture was stirred for 10 min. Dark green crystals of **5** suitable for X-ray diffraction were obtained after six days by slow evaporation, 60% yield. IR (KBr pellet, cm^{-1}): 1100(s), 1025(w), 960(s), 910(s). NMR of **5**. ^{31}P NMR: δ −9.34. Anal. calcd for **5**: Cu, 3.49; W, 50.50; Mo, 13.18; P, 1.42. Found: Cu, 4.01; W, 47.63; Mo, 11.50; P, 1.37.

$[(Cu(H_2O)_4)_{2.3}][H_{1.4}P_2W_{15}Mo_3O_{62}]\cdot 10.1H_2O$ (6). A total of 5 g (1.1 mmol) of $H_6P_2W_{15}Mo_3O_{62}$ was dissolved in 20 mL of water at room temperature. Solid $CuCl_2\cdot 2H_2O$ (0.572 g, 3.35 mmole) was then added. The mixture was stirred for 10 min. Green crystals of **6** suitable for X-ray diffraction were obtained after six days by slow evaporation, 65% yield. IR (KBr pellet, cm^{-1}): 1088(s), 1025(w), 959(s), 916(s). NMR of **6**. ^{31}P NMR: δ 0.80. Anal. calcd for **6**: Cu, 3.18; W, 60.01; Mo, 6.26; P, 1.35. Found: Cu, 3.47; W, 59.41; Mo, 6.16; P, 1.31.

$[(Co(H_2O)_4)_{2.3}][H_{1.4}P_2W_{14}Mo_4O_{62}]\cdot 18.8H_2O$ (7). A total of 5 g (1.2 mmol) of $H_6P_2W_{12}Mo_6O_{62}$ was dissolved in 20 mL of water at room temperature. Solid $CoCl_2\cdot 6H_2O$ (0.848 g, 3.56 mmol) was then added. The mixture was stirred for 10 min. Brown crystals of **7** suitable for X-ray diffraction were obtained after five days by slow evaporation, 65% yield. IR (KBr pellet, cm^{-1}): 1100(s), 1025(w), 960(s), 910(s). NMR of **7**. ^{31}P NMR: δ −10.10. Anal. calcd for **7**: Co, 2.91; W, 55.31; Mo, 8.25; P, 1.33. Found: Co, 2.98; W, 55.16; Mo, 7.60; P, 1.21

$[(Ni(H_2O)_4)_{1.85}][H_{2.3}P_2W_{15}Mo_3O_{62}]\cdot 20.6H_2O$ (8). A total of 5 g (1.1 mmol) of $H_6P_2W_{15}Mo_3O_{62}$ was dissolved in 20 mL of water at room temperature. Solid $NiCl_2\cdot 2H_2O$ (0.496 g, 3.35 mmole) was then added. The mixture was stirred for 10 min. Green crystals of **8** suitable for X-ray diffraction were obtained after five days by slow evaporation, 70% yield. IR (KBr pellet, cm^{-1}): 1088(s), 1025(w), 958(s), 915(s). NMR of **8**. ^{31}P NMR: δ 11.02. Anal. calcd for **6**: Ni, 3.18; W, 58.49; Mo, 6.10; P, 1.31. Found: Ni, 2.67; W, 58.50; Mo, 5.85; P, 1.25

Crystallographic Data Collection and Structure Determination. Single crystals were mounted on a Nonius four-circle diffractometer equipped with a CCD camera and a graphite monochromated Mo Kα radiation source (λ = 0.71073 Å), from the Centre de Diffractométrie (CDFIX), Université de Rennes 1, France. Data were collected at 293 K. Structures were solved by direct method using the SIR-97[19] program and refined with the full-matrix-least-squares method on F^2 using the SHELXL-97 program.[20] Several oxygen atoms from water solvent molecules were refined, but no SQUEEZE subroutine was used to remove the scattering from the remaining highly disordered water solvent molecules. Crystallographic data are summarized in Table 1.

Cyclic Voltammetry. Cyclic voltammetry experiments were performed on an EDAQ e-corder 401 potentiostat. All experiments were carried out using a three-electrode cell configuration with a glassy carbon working electrode, a saturated calomel reference electrode (SCE), and a platinum auxiliary electrode. All experimental solutions were deaerated thoroughly by bubbling pure N_2 through the solutions for 10 min. All cyclic voltammograms were recorded at a scan rate of 50 mV s^{-1}. All experiments were performed at room temperature.

(13) Abbessi, M.; Allal, K. M.; Bendjaballah, M.; Semar, M. E. *J. Soc. Alger. Chim.* **1994**, *4*, 1(C).
(14) Zabat, N.; Abbessi, M.; Kherrat, R.; Jaffrezic-Renault, N.; Grid, A. *Mater. Sci. Eng: C*. **2008**, *28*, 1006–1009.
(15) Contant, R.; Abbessi, M.; Thouvenot, R.; Hervé, G. *Inorg. Chem.* **2004**, *43*, 3597–3604.
(16) Park, D. R.; Kim, H.; Jung, J. C.; Lee, S. H.; Lee, J.; Song, I. K. *Catalysis Commun.* **2008**, *9*, 1312–1316.
(17) Ciabrini, J. P. Thèse de Doctorat es-Sciences, Université Pierre et Marie Curie, Paris VI, Paris, 1982.
(18) Ciabrini, J. P.; Contant, R.; Fruchart, J. M. *Polyhedron* **1983**, *2*, 1229–1233.
(19) Altomare, A.; Burla, M. C.; Camalli, M.; Cascarano, G. L.; Giacovazzo, C.; Guagliardi, A.; Moliterni, A. G. G.; Polidori, G.; Spagna, R. *J. Appl. Crystallogr.* **1999**, *32*, 115–119.
(20) Sheldrick, G. M. *SHELX-97*; University of Göttingen: Göttingen, Germany, 1997.

Results and Discussion

Synthesis IR and ^{31}P NMR Spectroscopy. The addition of Cu^{II} and Ni^{II} ions to Wells−Dawson acidic forms $[H_6P_2W_{18}O_{62}]\cdot 24H_2O$ or $[H_6P_2W_{18-n}Mo_nO_{62}]\cdot 24H_2O$ (n = 3, 6) in an aqueous medium, with a 3:1 stoichiometric amount, leads to a substitution of some protons by Cu^{II} and Ni^{II} ions, yielding crystals of the title compounds: $[(Cu(H_2O)_4)_{2.5}][HP_2W_{18}O_{62}]\cdot 11.33H_2O$ (**4**), $[(Cu(H_2O)_4)_{2.4}][H_{1.2}P_2W_{12}Mo_6O_{62}]\cdot 11.4H_2O$ (**5**), $[(Cu(H_2O)_4)_{2.3}][H_{1.4}P_2W_{15}Mo_3O_{62}]\cdot 10.1H_2O$ (**6**), $[(Co(H_2O)_4)_{2.3}][H_{1.4}P_2W_{14}Mo_4O_{62}]\cdot 18.8H_2O$ (**7**), and $[(Ni(H_2O)_4)_{1.85}][H_{2.3}P_2W_{15}Mo_3O_{62}]\cdot 20.6H_2O$ (**8**).

The addition of a 3:1 stoichiometric amount of Co^{II} to the acid form $H_6P_2W_{12}Mo_6O_{62}$ in an aqueous medium leads to powder and a few crystals of the compounds in which the Wells−Dawson transition metal ratio W/Mo is changed from 6:12 to 4:14 and some protons are substituted by Co^{II} ions: $[(Co(H_2O)_4)_{2.3}][H_{1.4}P_2W_{14}Mo_4O_{62}]\cdot 18.8H_2O$ (**7**). The presence of metals and their ratios are confirmed by electron scanning microscopy and X-ray diffraction. The IR spectrum of acidic Wells−Dawson compound $H_6P_2W_{18}O_{62}$ is characterized by the elongation of P−O bands at 1100 cm^{-1} and W−O terminal and *inter*- and *intra*-W−O−W bands at 960, 910, and 780 cm^{-1}, respectively.[21] However, the incorporation of transition ions in the structure generates a weak band at 1050 cm^{-1} attributed by Rocchioccioli-Deltchef and Thouvenot to a perturbation of one of the phosphorus atoms of the compound.[21] This means that the distribution of metallic ions is not equivalent around the two phosphorus atoms. It is well-known that phosphorus NMR is an appropriate and powerful way to check the purity of the product. Equivalence of the two phosphorus atoms is often because of a lack of coupling due to the remoteness of these atoms in the structure.[15] The NMR spectra of **4**, **6**, and **8** reveal pure products with two equivalent phosphorus atoms with single resonance peaks at δ = −12.36 ppm, δ = 0.80 ppm, and δ = 11.02 ppm, respectively.

^{31}P NMR of powder sample **5** gives two peaks, with a strong one at δ = −9.38 ppm which corresponds to the major compound $[(Cu(H_2O)_4)_{2.4}][H_{1.2}P_2W_{12}Mo_6O_{62}]\cdot 11.4H_2O$. The weak peak ($\delta$ = −10.16 ppm) must be assigned to $[P_2W_{14}Mo_4O_{62}]^{6-}$. Although the four atoms of molybdenum are not well-localized, the presence of one single peak in the ^{31}P NMR spectrum means that they are equivalently distributed around the two phosphorus atoms.

The ^{31}P NMR spectrum of **7** also reveals two peaks. In agreement with what is observed with their equivalent potassium salts,[17] the weak peak observed at δ = −10.10 ppm can be attributed to $[(Co(H_2O)_4)_{2.3}][H_{1.4}P_2W_{14}Mo_4O_{62}]\cdot 18.8H_2O$ and the strong one (δ = −9,34 ppm) to $[P_2W_{12}Mo_6O_{62}]^{6-}$. It is probably due to the partial degradation of the $[H_6P_2W_{12}Mo_6O_{62}]\cdot 24H_2O$ acid form in solution, followed by a recombination of W and Mo to give a well-crystallized species $[P_2W_{14}Mo_4O_{62}]^{6-}$ in equilibrium with the amorphous form $[P_2W_{12}Mo_6O_{62}]^{6-}$ species[17] and other compounds issued from decomposition. NMR spectra are presented in the Supporting Information.

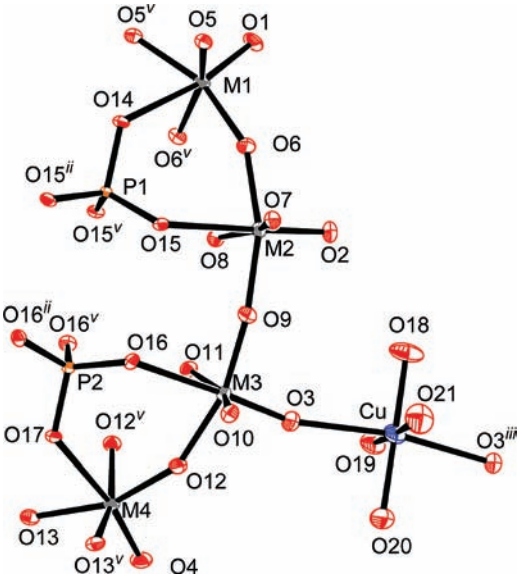

Figure 1. ORTEP view with 30% probability level of asymmetric unit of **4** with symmetry codes (ii) $2-y, 2+x-y, z$; (iii) $2-y, 2-x, z$; (v): $x, 2+x-y, z$. (M = W.)

Crystal Structures. Compounds 4, 5, and 6. Compounds **4**, **5**, and **6** are isostructural. They crystallize in the $R\bar{3}m$ space group; the refinements were performed in the related hexagonal axes. The asymmetric unit consists of two phosphorus atoms, four transition metal ions, and a Cu^{II} ion linked together by oxygen atoms (see Figure 1). In compound **4**, metallic sites are fully occupied by tungsten, giving rise to the $[P_2W_{18}O_{62}]^{6-}$ anion, whereas in **5** and **6**, statistic distribution between tungsten and molybdenum is observed for all metal sites. The occupation factors are about 1/3 W for M1 and M4 and 2/3 W for M2 and M3 for **5**. For **6**, the statistic disorder between tungsten and molybdenum is observed for only two sites (M1 and M4) with occupation factors of tungsten of 0.7 and 0.3, respectively; it corresponds to the occupation of the 3-fold cap of the complex by three molybdenums.[22] The remaining M2 and M3 sites are fully occupied by tungsten. Both phosphorus atoms P1 and P2 as well as oxygen atoms O14 and O17 are lying on the 6c Wyckoff position in 3m symmetry. Metallic atom sites M1, M2, M3, and M4 are lying in the middle of oxygen octahedra. Due to the space group symmetry, the six equivalent M2 and M3 atoms form two parallel distorted hexagonal $(M2)_6$ and $(M3)_6$ rings (see Figure 2). One can notice that O14 (and O17) is sharing three MO_6 octahedra and the PO_4 tetrahedron. The tetrahedral coordination sphere of the phosphorus atoms is completed with O15 (and O16) atoms, respectively, lying on the mirror plane of the 18h Wyckoff position. Both oxygen atoms O1, O4, O5, O7, O8, O10, O13 and metals M1 and M4 as well as the copper ion are also located on the 18h Wyckoff position.

Considering the molybdenum and tungsten radius differences (the M4 site is fulfilled at 70% with Mo), the bond distances and angles observed in the three compounds are homogeneous; they do not exceed a 1% difference. As commonly observed in Wells−Dawson

(21) Rocchioccioli-Deltchef, C.; Thouvenot, R. *Spectrosc. Lett.* **1979**, *12*, 127–138.

(22) Kozik, M.; Hammer, C. F.; Baker, L. C. W. *J. Am. Chem. Soc.* **1986**, *108*, 2748–2749.

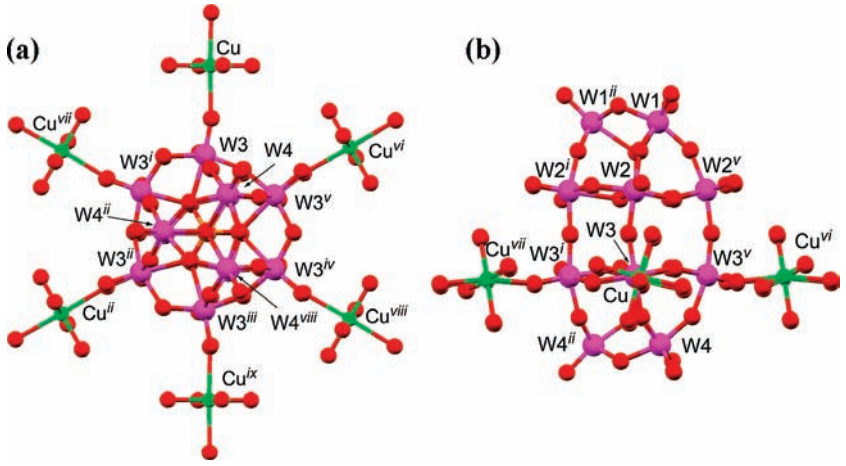

Figure 2. View of **4** (a) perpendicular and (b) along the polyoxometalate C_3 axis. Symmetry codes (i) $-x + y, y, z$; (ii) $2 - y, 2 + x - y, z$; (iii) $2 - y, 2 - x, z$; (iv) $-x + y, 2 - x, z$; (v) $x, 2 + x - y, z$; (vi) $1 - y, 2 + x - y, z$; (vii) $-x + y, 1 - x, z$; (viii) $-x + y, 2 - x, z$; (ix) $1 + x, 1 + y, z$.

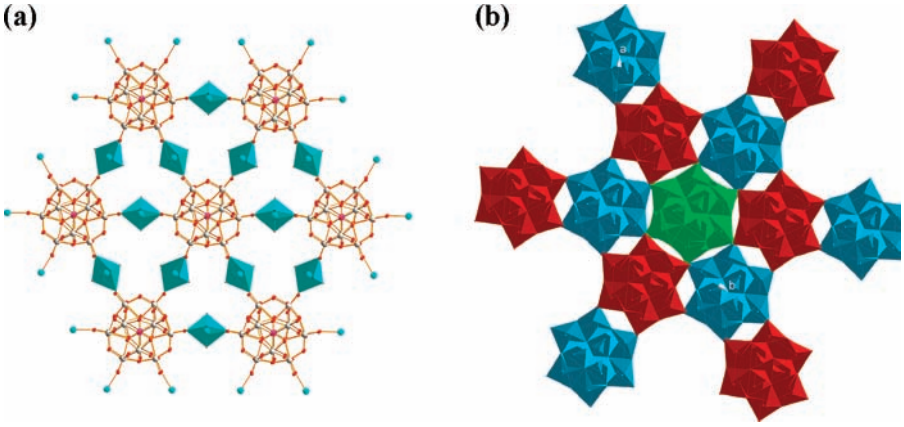

Figure 3. (a) Hexagonal packing of polyoxometalates onto the ab plane for **4**. (b) Packing of staggered ABC hexagonal network along the *c* axis. The B plane is drawn in blue polyhedra, and below and above this plane, there are two other staggered similar hexagonal planes, A in red and C in green.

polyoxometalates salts,[23] the shortest metal−oxygen bond distances are observed for terminal oxygen atoms (mean distances of 1.7135, 1.7045, and 1.6995 Å), whereas those involving oxygen atoms of PO_4 are the longest (2.3867, 2.3727, and 2.3687 Å) for **4**, **5**, and **6**, respectively. Mean M−O bond distances involving other oxygen atoms are found to be equal to 1.919, 1.920, and 1.910 Å for **4**, **5**, and **6** respectively. All bond distances are given in Table S1 (Supporting Information); acute O−M−O angles involving adjacent bridging O's range from 72.39(19) to 89.6(2)°.

The copper ion is lying at the center of an octahedral oxygen coordination sphere, slightly Jahn−Teller-distorted. The apical positions are filled with O3 oxygen atoms belonging to the polyanion with Cu−O3 distances equal to 2.432(5), 2.438(6), and 2.421(5) Å for **4**, **5**, and **6**, respectively. The octahedron is completed with four oxygen atoms from water molecules. The occupation factors of both Cu and O atoms within the $[CuO_2(H_2O)_4]$ octahedron were assumed to ride together and were found equal to be 0.417, 0.404, and 0.370. The equatorial square plane is quite regular for **4**, with Cu−O bond distances ranging from 1.968(9) to 1.978(9) Å, while it is less regular for **5** and **6**, with distances ranging from 1.959(11) to 1.983 (11) and from 1.938(13) to 1.957(12) Å, respectively. In the *ab* plane, each Wells−Dawson anion unit is bridged to six other polyoxometalates and bridged via six copper ions.

In the *ab* plane, each Wells−Dawson anion unit is bridged to six other neighboring ones via six copper ions, leading to a hexagonal 2D network (see Figure 3).

Compounds 7 and 8. Both compounds crystallize in the $P\bar{1}$ triclinic space group. Crystal data are given in Table 1. The asymmetric unit of both compounds consists of one Wells−Dawson $[P_2W_{18-n}Mo_nO_{62}]^{6-}$ polyoxometalate (n = 4 and 3 for **7** and **8**, respectively), 3d transition metal ions surrounded by water molecules, and free water solvent. Despite the two unit cell parameters of both **7** and **8** being quite similar, large differences can be observed between their structures, especially concerning the Mo substitution sites. As commonly observed for Wells−Dawson polyoxometalates, two kinds of metal−metal distances through one oxygen are observed: the short ones are of about 3.4−3.5 Å, the others are found to be around 3.7−3.8 Å. One can notice that it is possible to build three M_6 units as elongated hexagonal cycles with a boat conformation with all M−M distances within the cycle of about 3.7 Å. These cycles surround the two central phosphorus ions, and all of the M−M distances

(23) D'Amour, H. *Acta Crystallogr.* **1976**, *B32*, 729–740.

Table 1. Crystallographic Data

compound	4	5	6	7	8
empirical formula	$P_2W_{18}O_{83.33}H_{43.66}Cu_{2.5}$	$P_2W_{12}Mo_6O_{83}H_{43.2}Cu_{2.42}$	$P_2W_{15}Mo_3O_{81.33}H_{40}Cu_{2.3}$	$P_2W_{14}Mo_4O_{90}H_{57.4}Co_{2.3}$	$P_2W_{15}Mo_3O_{90}H_{58.3}Ni_{1.85}$
fw	4907.44	4369.02	4595.31	4653.00	4714.89
cryst syst	trigonal	trigonal	trigonal	triclinic	triclinic
space group	$R\bar{3}m$	$R\bar{3}m$	$R\bar{3}m$	$P\bar{1}$	$P\bar{1}$
a (Å)	15.2890(9)	15.2387(9)	15.1940(11)	13.125(2)	12.9160(10)
b (Å)	15.2890(9)	15.2387(9)	15.1940(11)	14.8355(17)	14.6630(10)
c (Å)	55.9800(10)	56.1227(10)	55.6570(10)	21.072(8)	20.9770(10)
α (deg)	90	90	90	84.609(19)	84.956(10)
β (deg)	90	90	90	88.62(2)	88.707(10)
γ (deg)	120	120	120	66.763(10)	66.299(10)
V (Å^3)	11332.4(10)	11286.6(10)	11127.4(12)	3753.0(16)	3623.3(4)
Z	6	6	6	2	2
D_{calcd} (g cm^{-3})	4.314	3.856	4.115	4.117	4.328
μ (mm^{-1})	28.130	20.055	24.418	22.670	24.890
R_1[a]	0.0316	0.0441	0.0411	0.0503	0.0454
wR_2[b]	0.0597	0.0897	0.1054	0.1166	0.1050

[a] For reflections where $I > 2\sigma(I)$ with $R_1 = \sum||F_o| - |F_c||/\sum|F_o|$. [b] For reflections where $I > 2\sigma(I)$ with $wR_2 = \{\sum[w(F_o^2 - F_c^2)^2]/\sum[w(F_o^2)^2]\}^{1/2}$.

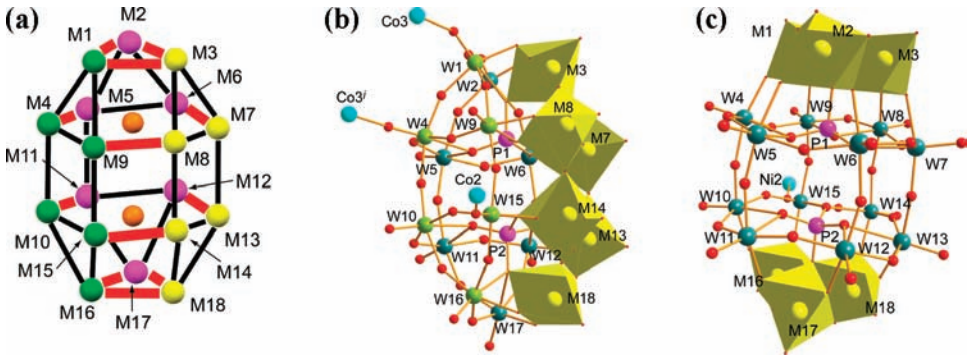

Figure 4. (a) Metal site standard labeling scheme of metal position in Wells−Dawson polyoxometalate, with short-distance (3.4−3.55 Å) contacts in bold lines and long distances (3.7−3.8 Å) in thin lines. (b, c) Labeling scheme of polyoxometalate in **7** and **8**, respectively (i: $1-x, 1-y, 2-z$). Metallic sites fully occupied with tungsten are drawn as balls and sticks; the centers of octahedra are statistically occupied with tungsten and molybdenum.

between M_6 cycles are of about 3.4 Å. Figure 4a gives the details of the 18 metal positions of the Wells−Dawson polyoxometalate.

In both compounds, 12 of the 18 transition metal positions are fully occupied with tungsten atoms, whereas the six remaining metal positions are statistically occupied with tungsten and molybdenum ions, but the location of the six tungsten ions differs (see below). In both compounds, all MO_6 octahedra present a short bond distance from the metal to the terminal oxygen atom (from 1.686(9) Å to 1.749(10) Å in **7**; from 1.674(8) to 1.723 (10) Å in **8**) and a long bond distance involving the O atom of PO_4^{3-} anions (from 2.338(9) to 2.413(8) Å and from 2.320(7) to 2.421(7) Å, respectively] in the opposite vertex of the octahedron. The O−M−O angles range from 168.8(4)° to 174.2(4)° [170.1(3)° to 173.6(4)°]. All of the other M−O bond lengths are in the same range with a mean value of 1.930 [1.909] Å (from 1.806(8) to 2.114(8) Å [1.839(9) to 2.016(7) Å]). As reported in tungsten-based Wells−Dawson polyoxometalates, no alternating M−O short and long bond length distortions are observed.[24]

Compound $[(Co(H_2O)_4)_{2.3}][H_{1.4}P_2W_{14}Mo_4O_{62}]\cdot 18.8H_2O$ (7). The four molybdenum ions are delocalized onto the six positions of one single M_6 cycle (see Figure 4b) with occupation factors ranging from 0.614(5) to 0.679(5) for M3 and M13, respectively; the mean value for tungsten atom is 0.65(2). The octahedra involving Mo are less regular than WO_6 octahedra; the range of W−O bond lengths (excluding terminal and central oxygen) is reduced to 1.849(8)−2.014(8) Å. Three sites in general positions are fulfilled with a 3d transition metal (M″1, M″2, and M″3); their occupation factors were found respectively to be equal to 1, 0.383, and 0.934, yielding 2.3 cobalt ions per Wells−Dawson anion. Each ion is surrounded by six oxygen atoms, but each one has its own coordination molecules. M″1 is lying in the structure as a free hexa-aquo ion, surrounded with six water molecules. M″2 is bonded to one Wells−Dawson ion through its terminal oxygen O15, and five oxygens from water solvent molecules complete its octahedral coordination sphere. M″3 is bridging three polyoxometalates thanks to O1, O4, and O16 terminal atoms; its octahedral coordination sphere is completed with three water molecules. The Co−O bond distances are quite homogeneous for Co1 and Co2 with a mean bond distance Co−O of 2.105 Å (see Table S2, Supporting Information). Co3 adopts an elongated octahedral geometry with an elongation axis determined by oxygen atoms O1 and O4^i. As the opposite vertexes O1 and O4^i of $Co3O_3(H_2O)_3$ are the terminal oxygen atoms of two Wells−Dawson polyanions, Co3 acts as a bridging metal between them.

(24) Yan, L.; López, X.; Carbó, J. J.; Sniatynsky, R.; Ducan, D. C.; Poblet, J. M. *J. Am. Chem. Soc.* **2008**, *130*, 8223–8233.

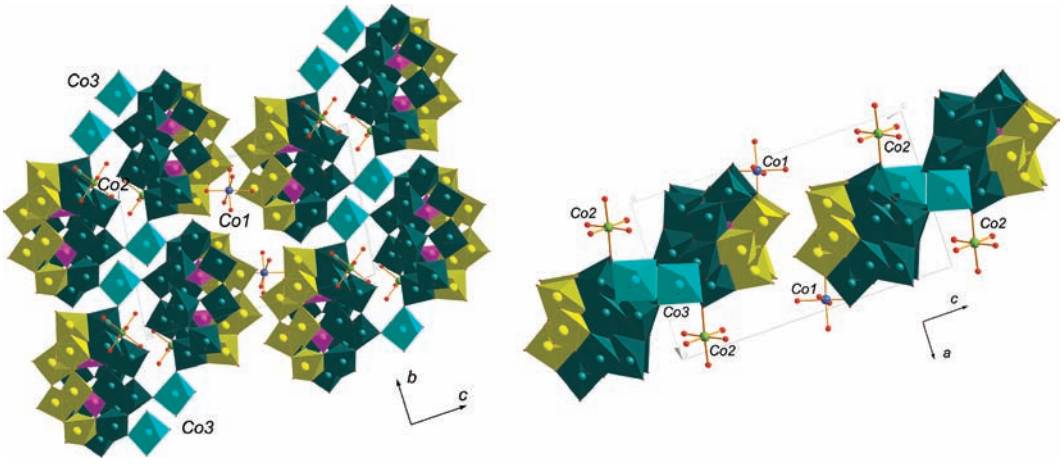

Figure 5. Polyhedral representation of **7**: (a, left) two ribbons in the (201) plane build of polyanions connected with Co3 cations, (b, right) the same two-ribbons view along the *b* axis.

Furthermore, in one Wells−Dawson polyanion, the two terminal oxygen atoms O1 and O4 belong to two close WO_6 octahedra, which share one of their vertices. Due to these geometrical reasons, the two polyanions are, in fact, bridged with two Co3 cations. The last oxygen atom of the $Co3O_3(H_2O)_3$ unit, labeled $O16^{ii}$, is also bridging a third polyanion. This packing yields along the *b* direction an infinite double chain of polyanions bridged with a Co3 cation (see Figure 5). This double chain forms a kind of ribbon parallel to the (2 0 1) plane. One can notice that the W/Mo positions are lying in the border of the ribbon (Figure 5). The $Co2O_5(H_2O)$ octahedra are linked above and below this ribbon, and $Co1(H_2O)_6$ is located between the ribbons.

Compound $[(Ni(H_2O)_4)_{1.85}][H_{2.3}P_2W_{15}Mo_3O_{62}]\cdot 20.6H_2O$ (8). As commonly observed in $P_2M_{15}M'_3$ Wells−Dawson polyanions, the six W atoms statistically occupy six M″ sites in the two opposite triads, with a W/Mo occupation factor of ca. 0.5 (octahedra in Figure 4c). Only 1.85 ions of nickel were found per Wells−Dawson in **8**, and only M″1 and M″2 positions are fulfilled with nickel ions, with occupation factors of about 0.933 and 0.917, respectively. A low electronic density was observed for the third position M″3, but it was not possible to affect a nickel ion. The Ni−O bond distances are quite homogeneous with a mean bond distance of 2.028 Å. Additionally, as shown in Figure 6, there exists a strong hydrogen bond network involving free water molecules, the two $Ni(H_2O)_4$ cations, and the terminal oxygen atoms from the Wells−Dawson.

Cyclic Voltammetry. The following study is restricted to the reversible redox processes for compound **4**, **5**, **6**, and **8** and their pH dependencies.[5,25−28]

Compound $[(Cu(H_2O)_4)_{2.5}][HP_2W_{18}O_{62}]\cdot 11.33H_2O$ (4). The cyclic voltammetry data of **4** at pH = 3 show reductions over the range −0.1 to −1 V/SCE and oxidations

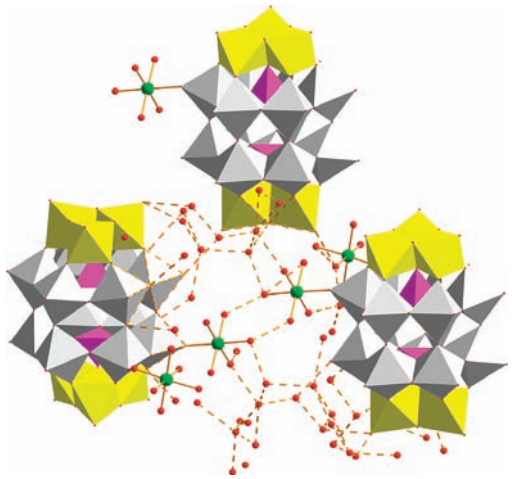

Figure 6. Structural arrangement in **8** with hydrogen-bonding network.

over the range −0.7 to +0.3 V. These results are in agreement with the previous studies on heteropolyanion electrochemistry.[26,28] In Figure 7a, at pH = 3, the voltammogram shows three redox systems. The first wave situated at −0.15 V/SCE is assigned to the reduction of the copper. The waves corresponding to the reduction of tungsten appear at 0.6 and 0.85 V/SCE. The reduction wave of copper is well-separated from the tungsten wave reduction. Upon reduction, a deposition process on the working electrode is observed for the Cu^{II} complexes.[25−27] Subsequently, after oxidation of the copper film, the initial complex is restored quantitatively.[26] At pH 5, the reduction of copper is performed in two steps, and the reduction wave of tungsten moves in the positive direction of potentials.

$[(Cu(H_2O)_4)_{2.4}][H_{1.2}P_2W_{12}Mo_6O_{62}]\cdot 11.4H_2O$ (5). The cyclic voltammetry data of **5** at pH = 3 show reductions over the range +0.5 to −0.8 V/SCE and oxidation over the range −0.7 to 0.6 V/SCE.[29] As shown in Figure 7b, the voltammogram shows five redox systems. In heteropolyanions, molybdenum is reduced before tungsten, and if we refer to the voltammogram of **4**, the

(25) Keita, B.; Lu, Y. W.; Nadjo, L.; Contant, R.; Abbessi, M.; Canny, J.; Richet, M. *J. Electronal. Chem.* **1999**, *477*, 146–157.
(26) Contant, R.; Abbessi, M.; Canny, J.; Richet, M.; Belhouari, A.; Keita, B.; Nadjo, L. *J. Inorg. Chem.* **2000**, *3*, 567–574.
(27) Keita, B.; Abdeldjalil, E.; Nadjo, L.; Avisse, B.; Contant, R.; Canny, J.; Richet, M. *Electrochem. Commun.* **2000**, *2*(3), 145–149.
(28) Keita, B.; Abdeljalil, E.; Nadjo, L.; Contant, R.; Belghiche, R. *Electrochem. Commun.* **2001**, *3*, 56–62.
(29) Tommasino, J. B.; Contant, R.; Michet, J. P.; Roncin, J. *Polyhedron* **1998**, *17*, 357–366.

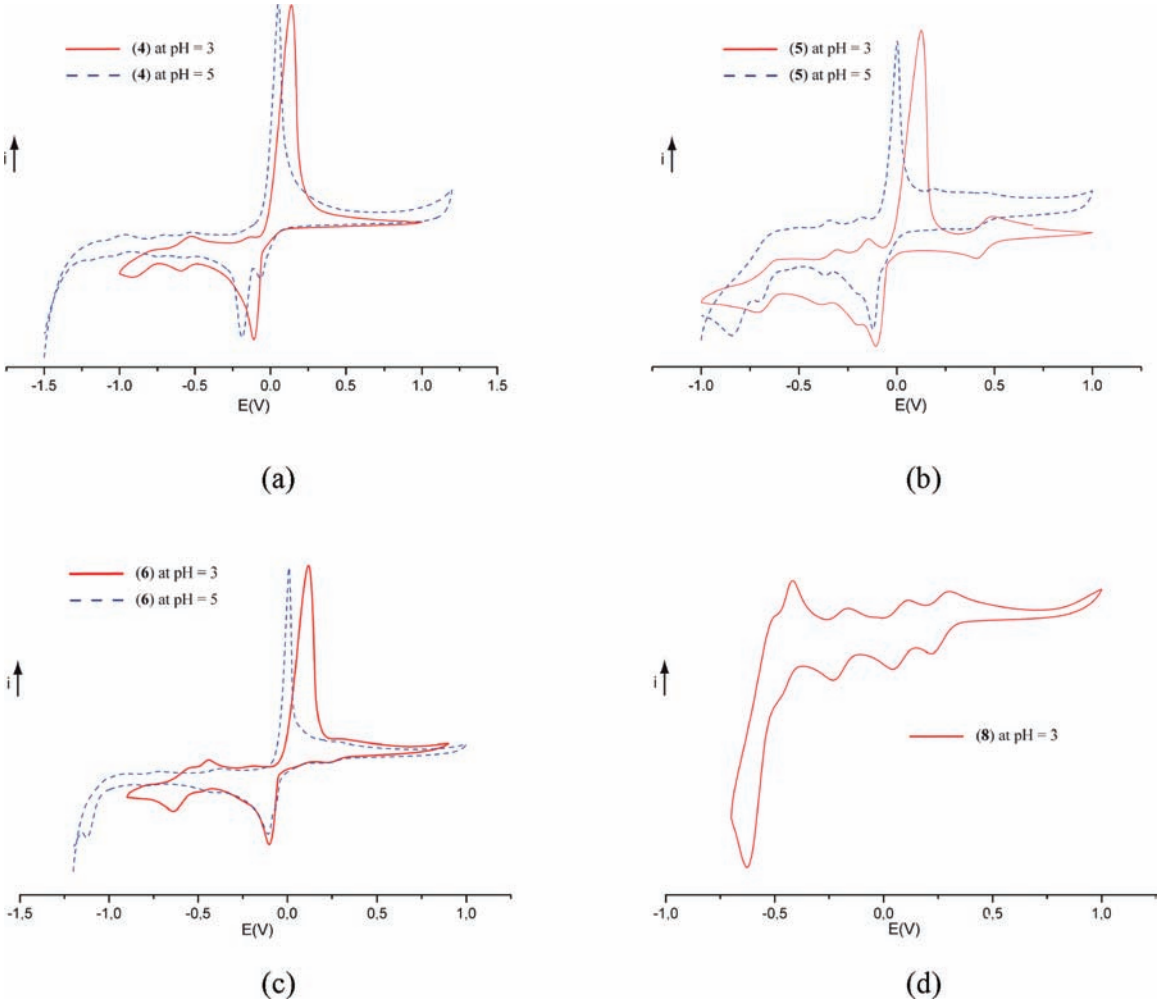

Figure 7. Cyclic voltammograms on Pt working electrode vs SCE, scan rate 50 mV s^{-1}, for 10^{-3} solutions of (a) compound **4** at pH = 3 and pH = 5, (b) compound **5** at pH = 3 and pH = 5, (c) compound **6** at pH = 3 and pH = 5, and (d) compound **8** at pH = 3.

first wave situated at 0.42 V/SCE is assigned to the reduction of molybdenum atoms. The second wave situated at −0.15 V/SCE characterizes the reduction of copper. The last three waves correspond to the reduction of tungsten. At pH = 5, the Mo and W centers are more easily reducible than at pH = 3. This is due to the presence of a high Mo/W ratio, as already observed for related compounds.[30]

$[(Cu(H_2O)_4)_{2.3}][H_{1.4}P_2W_{15}Mo_3O_{62}]\cdot 10.1H_2O$ (6). The cyclic voltammetry data of **6** at pH = 3 show reductions over the range +0.3 to −0.7 V/SCE and oxidations over the range −0.6 to +0.1 V/SCE. The voltammogram shows three redox systems. The first wave situated at 0.25 V/SCE is assigned to the reduction of molybdenum atoms. The second wave situated at −0.1 V/SCE is attributed to the reduction of copper. The third wave corresponds to the reduction of the tungsten atom. For tungsten, two reoxidation waves are observed. On the other hand, the reoxidation wave of molybdenum is not observed. So, molybdenum and copper are reoxidized simultaneously. The same behavior is observed at pH = 5, which is in agreement with the reported data.[4]

In **5**, the oxidation wave of molybdenum is well-separated from the copper oxidation wave, in contrast to the waves observed for **6**.

$[(Ni(H_2O)_4)_{1.85}][H_{2.3}P_2W_{15}Mo_3O_{62}]\cdot 20.6H_2O$ (8). The cyclic voltammetry data of **8** at pH = 3 show redox systems over the range −0.6 to +1 V/SCE. The voltammogram shows the same redox systems as those observed for the starting compound. Thus, Ni^{2+} undergoes no redox reaction in the explored range. At both pH = 3 and pH = 5, copper reduction occurs at the same potential for **5** and **6** and slightly shifted to negative potentials for **4**. As usual, in the Ni-containing POM,[4] we did not observe the Ni redox system for **8** in the potential domain that we explored.

Conclusion

Five new heteropolyanions with the general formula $[(M(H_2O)_4)_x][H_{6-2x}P_2W_{18-n}Mo_nO_{62}]\cdot zH_2O$ (M = Cu^{II}, Co^{II}, Ni^{II}) have been synthesized in an aqueous medium, from acid forms of their related saturated species and metallic ions. Structural determinations revealed that **4**, **5**, and **6** are isostructural, as are **7** and **8**. Different kinds of Mo substitutions are observed in **5** and **6**; the Mo atoms are statistically distributed over all 18 of the metal sites of the polyanion. In **8**, the Mo atoms are distributed on the opposite top and bottom

(30) Keita, B.; Girard, F.; Nadjo, L.; Contant, R.; Belghiche, R.; Abbessi, M. *J. Electroanal. Chem.* **2001**, *508*, 70–80.

M_3 triads, while in **7**, the substitution takes place on the side M6 hexagon. ^{31}P NMR and X-ray diffraction showed that, under our reaction conditions, the reaction of the acid form and Co^{II} leads to $[(Co(H_2O)_4)_{2.3}][H_{1.4}P_2W_{14}Mo_4O_{62}]\cdot 18.8\ H_2O$ (**7**), following a rearrangement within the heteropolyanion. The crystal structures of **4**, **5**, and **6** consist of 2D polymeric hexagonal layers where each Wells−Dawson anion is connected to six neighbors by $[CuO_6]$ octahedra, whereas compounds **7** and **8** have a 3D structure where the Mo-substituted $[P_2W_{14}Mo_4O_{62}]$ units are connected by $[MO_6]$ octahedra M = Co^{II} and Ni^{II}, respectively. Additionally, a strong hydrogen-bonding network exists in compound **8**.

The cyclic voltammetry analysis showed that copper-containing compounds **4**, **5**, and **6** have redox behavior different from their precursors, while nickel compound **8** and the initial compound have the same one. The decomposition process has been observed for Cu salts. From pH = 5 to pH = 3, the copper wave is shifted to higher positive potentials.

Acknowledgment. This work is supported by the Algerian Ministry of Education and Research, the University of Annaba, the University of Rennes 1, the CNRS, and the Région Bretagne. We thank Dr. J.-F. Halet, UMR 6226, University of Rennes 1, for helpful discussions.

Supporting Information Available: Plots of IR and NMR; ORTEP drawing of the polyanion in **7**; selected bond distances for **4**, **5**, and **6**; and selected lengths and angle for **7** and **8**, as well as crystallographic information files (CIF). These materials are available free of charge via the Internet at http://pubs.acs.org.